Volume 3, Number 1 ACTA PHYSICA SINICA January, 1994
1004-423X/94/03010051-05 (Overseas Edition) © 1994 Science Press

EFFECTS OF THE HUBBARD INTERACTIONS AND ELECTROSTATIC PINNING ON THE 2D LOCALIZED MODES OF TRANS-$(CH)_x$ AROUND A SOLITON*

YAO KAI-LUN(姚凯伦) and LI ZHAN-JIE(李占杰)
Department of Physics, Huazhong University of Science and Technology, Wuhan 430074, China
XING BIAO(邢 彪)
Department of Physics, University of Alberta Edmontan, Canada 76G 2J1

(Received 13 April 1993)

The electron-lattice coupling vibrational modes are calculated using a two-dimensional extension of the Su-Schrieffer-Heeger model that includes the bond-bending term, the electron-electron interactions and the electrostatic pinning for doped samples. The result shows that all ten localized modes exist after turning on the e-e interactions and doped pinning effects, but their localizations has been strengthened and the frequencies have been moved slightly.

PACC: 6320P; 7280L

In order to interpret the infrared absorption experiments, the localized vibrational modes have been studied based on both Su-Schrieffer-Heeger(SSH) model[1] or its continuum version Takayama-Lin-Liu-Maki(TLM) model[2], which will smear out staggered modes with rapidly varying configuration. In single pure samples of polyacetylene, Ito, Terai, Ono and Wada[3,4] have found three localized modes for a soliton and five for a polaron from TLM model. By using the SSH model, *Sun et al*[5,6], have gotten four soliton-related localized modes and seven polaron-related modes. Besides, the present authors have assessed the influence of polyacetylene configuration on the localized vibrational modes around a polaron or a soliton from the two-dimensional extension of SSH model[7-9]. The results show that the vibrations normal to the $(CH)_x$ chain and along the chain become comparable for most modes, when the in-plane degrees of freedom are included. Several additional localized modes have been found, compared with that in SSH model. However, in these works, the electron-electron interactions and the pinning effects were ignored. So, we will continue our investigations based on previous papers[8], where the e-e interactions and electrostatic pinning effects are considered.

Instead of one-dimensional SSH model, we start from the two-dimensional extension of the SSH model and investigate the small oscillation around a soliton.

The model Hamiltonian is given as

$$H = -\sum_{n,\sigma}(t_0 - \alpha\delta r_{n+1,n})(c^+_{n+1,\sigma}c_{n,\sigma} + \text{H.c.}) + \frac{k}{2}\sum_n(\delta r_{n+1,n})^2 + \frac{k'}{2}\sum_n(\delta\theta_n)^2 + \sum_n v(n) - \sum_{n,\sigma} v(n)c^+_{n,\sigma}c_{n,\sigma} + \frac{1}{2}U\sum_{n,\sigma} c^+_{n,\sigma}c_{n,\sigma}c^+_{n,-\sigma}c_{n,-\sigma} + \frac{M}{2}\sum_n(\dot{r})^2 , \quad (1)$$

*Project supported by the National Natural Science Foundation of China.

where t_0, α, k and M have the same conventional meanings as in the SSH model; k' is the spring constant of the bond-bending term; $\delta r_{n+1,n}$ denotes the change of bond-length from the equilibrium position between the nth site and the $(n+1)$th site. U is the interaction parameter of Hubbard repulsion, $v(n)$ is the Coulomb potential of the pinning charge, which is taken as a point charge for the doped samples[10,11].

$$v(n) = -\frac{e^2\exp(\rho R_n)}{\varepsilon_1^{1/2}\varepsilon_2 R_n}\ , \tag{2}$$

where ρ is chosen to fit the experimental data and found to be 5.9/nm, R_n is the distance from the nth site of the chain to the off-chain dopant, ε_1 and ε_2 are dielectric constants parallel and perpendicular to the chain, and equal to 7.1 and 1.8, respectively.

$$R_n^2 = \frac{(n-(n+1)/2)^2 a_0^2}{\varepsilon_1} + \frac{d_0^2}{\varepsilon_2}\ , \tag{3}$$

here a_0 is the distance between carbon sites and equals to 0.123 nm, d_0 is the distance of the charged impurity from the chain and equals to 0.21 nm.

Introducing the dimensionless parameters

$$\delta u_{n+1,n} = \frac{\alpha}{t_0}\delta r_{n+1,n},\quad \lambda = \frac{2\alpha^2}{\pi k t_0},\quad \tau = \omega_Q t,\quad k'' = k'/t_0,\quad \gamma = U/t_0\ , \tag{4}$$

where $\omega_Q = (4k/M)^{1/2}$ is the bare frequency, then Hamiltonian can be written as

$$\begin{aligned} H/t_0 = &-\sum_{n,\sigma}(1-\delta u_{n+1,n})(c^+_{n+1,\sigma}c_{n,\sigma} + \text{H.c.}) + \frac{1}{\lambda\pi}\sum_n(\delta u_{n+1,n})^2 + \frac{k''}{2}\sum_n(\delta\theta_n)^2 \\ &+ \sum_n v'(n) - \sum_{n,\sigma} v'(n)c^+_{n,\sigma}c_{n,\sigma} + \frac{1}{2}\gamma\sum_{n,\sigma} c^+_{n,\sigma}c_{n,\sigma}c^+_{n,-\sigma}c_{n,-\sigma} + \frac{4}{\lambda\pi}\sum_n(\dot{u}_n)^2\ , \end{aligned} \tag{5}$$

where $\dot{u}_n = \frac{du_n}{d\tau}$ and $v'(n) = v(n)/t_0$. A static solution of soliton can be determined by the following self-consistent equations which is irrelevant to the bond-bending term:

$$\begin{aligned} \varepsilon_i^\sigma\psi_i^\sigma(n) &= -(1-\delta u_{n,n-1})\psi_i^\sigma(n-1) - (1-\delta u_{n+1,n})\psi_i^\sigma(n+1) + (v(n)+\gamma\chi_{n,\sigma})\psi_i^\sigma(n)\ , \\ \chi_{n,\sigma} &= \sum_{\substack{i\\(\text{occ})}}\psi_i^{-\sigma}(n)\psi_i^{-\sigma}(n)\ , \\ \delta u_{n+1,n} &= -\lambda\pi\sum_{\substack{i\\(\text{occ})}}\psi_i(n+1)\psi_i(n) + \xi\ , \end{aligned} \tag{6}$$

where the open chain boundary condition has been used. ε_i^σ is the eigenvalue of electron with spin σ, and $\psi_i^\sigma(n)$ denotes the nth component of electron eigenfunction with spin σ.

Now, we consider the small vibration around soliton, expanding $\delta u_{n+1,n}$ near the equilibrium configuration $\{\delta u^s_{n+1,n}\}$[7,8]

$$\delta u_{n+1,n} = \sin\theta(x_{n+1}-x_n) + (-1)^{n+1}\cos\theta(y_{n+1}-y_n) + \delta u^s_{n+1,n}\ , \tag{7}$$

where θ is half of the bond angle and coordinate is chosen as in Ref. [7]. The direction of chain is defined as x, and the normal direction is y. Then the total energy can be written as

$$E = E^s + \frac{1}{2}\sum_{m,n} v_{mn}^{\alpha\beta}\eta_m^\alpha\eta_n^\beta + \frac{4}{\lambda\pi}\sum_n (\dot{u}_n)^2 \ , \tag{8}$$

where α, $\beta = 1, 2$ denote x direction and y direction, respectively. E^s is the energy of the soliton.

$$\eta_m^1 = x_m, \quad \eta_m^2 = y_m \ ,$$

$$v_{mn}^{\alpha\beta} = 2\sum_{\substack{i,\sigma \\ (\mathrm{occ})}}\sum_{j\neq i}\frac{D_{ij}^{m\alpha}D_{ij}^{n\beta}}{\varepsilon_i - \varepsilon_j} - 2\sum_{k,l,\sigma} B_{m,k}^\alpha (G^{-1})_{k,l} B_{n,l}^\beta + M_{mn}^{\alpha\beta} + M_{mn}^{\prime\alpha\beta} \ , \tag{9}$$

$$D_{ij}^{n\alpha} = c_{ij}^n q_n^\alpha (1-\delta_{n1}) - c_{ij}^{n+1} q_{n+1}^\alpha (1-\delta_{nN}), \quad q_n^1 = \sin\theta, \quad q_n^2 = (-1)^n \cos\theta \ ,$$

$$c_{ij}^n = \psi_i(n)\psi_j(n-1) + \psi_j(n)\psi_i(n-1) \ ,$$

$$G_{mn} = \sum_{\substack{i,j \\ (j\neq i)}} \frac{A_{ij}^m A_{ij}^n}{\varepsilon_i - \varepsilon_j} - \frac{1}{2\gamma}\delta_{mn} \ , \tag{10}$$

$$B_{mn}^\alpha = \sum_{\substack{i,j \\ (j\neq i)}} \frac{D_{ij}^{m\alpha} A_{ij}^n}{\varepsilon_i - \varepsilon_j}, \quad A_{ij}^n = \psi_i(n)\psi_j(n) \ , \tag{11}$$

where G^{-1} is the inverse matrix of $\{G_{mn}\}$, $M_{mn}^{\alpha\beta}$ and $M_{mn}^{\prime\alpha\beta}$ denote the bond-stretching energy and bond-bending energy, respectively. Readers are referred to Ref. [8, 9] for their explicit expressions.

For a charge soliton, we take a chain of 101 atoms with 100 electrons. The parameters are $t_0 = 2.5\,\mathrm{eV}$, $\alpha = 4.16\,\mathrm{eV/nm}$, $K = 2100\,\mathrm{eV/nm^2}$, k'=1.625 eV, and we have found $\xi = 0.412$. One can obtain all the vibrational modes by diagonalizing the matrix $\{V_{mn}\}$. The vibrational amplitude G_i corresponding to the frequency ω_i can be expressed as

$$G_i = \{G_i^x, G_i^y\} = (X_1^i \cdots X_m^i \cdots X_{101}^i, Y_1^i \cdots Y_m^i \cdots Y_{101}^i) \ , \tag{12}$$

where X_m^i and Y_m^i stand for the vibrational amplitudes of the mth site in the X and Y direction, respectively.

Now, we turn to a discussion of the results of numerical calculation. Ten localized modes, which have been obtained without e-e interactions and pinning effects, always survive (see Table 1). Among these modes, G_2 (Goldstone mode), G_3, G_4 and G_6 (staggered mode) have

Table 1. Frequencies of the localized modes around a soliton for different γ.

Localized modes	Frequencies ω_i/ω_Q				
	$\gamma = 0.0$	$\gamma = 0.2$	$\gamma = 0.5$	$\gamma = 0.8$	$\gamma = 1.0$
G_1	0.2259	0.2260	0.2261	0.2262	0.2271
G_2	0.3322	0.3290	0.3208	0.3175	0.3135
G_3	0.4855	0.4837	0.4817	0.4790	0.4775
G_4	0.5384	0.5379	0.5361	0.5359	0.5352
G_5	0.6373	0.6372	0.6369	0.6368	0.6371
G_6	0.6365	0.6367	0.6377	0.6378	0.6380
G_7	0.6149	0.6157	0.6169	0.6171	0.6772
G_8	0.6388	0.6386	0.6384	0.6382	0.6382
G_9	0.6403	0.6402	0.6401	0.6399	0.6399
G_{10}	0.6704	0.6705	0.6708	0.6708	0.6709

their correspondents in the one-dimensional results according to the shapes of the X amplitudes. The modes G_1, G_5 and $G_7 - G_{10}$ are the additional ones, compared with the four modes of the SSH model. The X and Y amplitudes of these modes have the inverse symmetry about the center of the chain, and the amplitudes of both directions for most modes are comparable to our previous results[8,9]. The modes G_2, G_4 and G_5 are IR active, related to infrared absorption.

The results show that the frequencies for modes G_2, G_9, G_4, G_5, G_8 and G_9 slightly decrease when the parameter γ increases, but the modes G_1, G_6, G_7 and G_{10} have the opposite behaviors. Furthermore, the localization is strengthened with the increasing e-e interactions. The shape of mode G_{10} is shown for $\gamma = 0.0$, 1.0 in Figs. 1 and 2. Besides, for pinning in chemically doped systems, the electrostatic pinning effects only change the frequencies of the modes and their localizations as in the SSH model[10,11]. Thus our conclusion is that the number of localized modes depends on the coupling constant λ and the spring constant k'[8], the electron-electron interactions and the pinning effects only cause shifts of frequencies and strengthening of localizations.

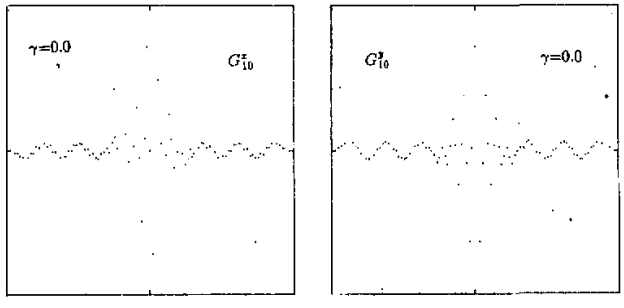

Fig. 1. The shape of the localized mode G_{10} for $\gamma = 0.0$. The unit of the abscissa is site number n, and the ordinate is in an arbitrary unit.

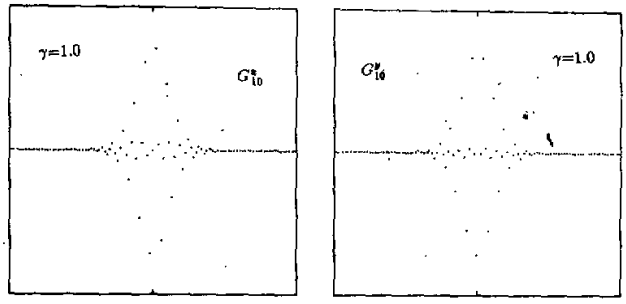

Fig. 2. The shape of the localized mode G_{10} for $\gamma = 1.0$. The units of both axes are the same as in Fig.1.

Finally, we would like to make some comparison of our results with the experimental data, while the G_2 (Goldstone mode) corresponding to $900\,\mathrm{cm}^{-1}$, the modes G_4 and G_5 (additional modes) accord with observed infrared absorption peaks at 1260, $1370\,\mathrm{cm}^{-1}$ [12], respectively. For polyacetylene, the exact values of parameters λ, k' and U are unclear. In order to get more precise results, we will make a further computation with real parameters.

REFERENCES

[1] P. W. Su, J. R. Schrieffer and A. J. Heeger, *Phys. Rev.*, **B22** (1980), 2099.
[2] H. Takayama, Y. R. Lin-Liu and K. Maki, *Phys. Rev.*, **B21** (1980), 2388.
[3] H. Ito *et al.*, *J. Phys. Soc. Jpn.*, **53** (1984), 3519.
[4] A. Terai and y. Ono, *J. Phys. Soc. Jpn.*, **55** (1986), 213.
[5] X. Sun, C. Wu and X. Shen, *Solid State Commun.*, **56** (1985), 1039.
[6] X. Sun *et al.*, *Phys. Rev.*, **B35** (1987), 4102.
[7] Biao Xing and K. L. Yao, *Phys. Rev.*, **B42** (1990), 2085.
[8] Z. J. Li, Biao Xing and K. L. Yao, *Phys. Rev.*, **B44** (1991), 5029.
[9] K. L. Yao, Z. J. Li and Biao Xing, *Acta Phys. Sin.*, **41** (1992),87.
[10] Richard J. Cohen and Arnold J. Glick, *Phys. Rev.*, **B36** (1987), 2907.
[11] J. C. Hicks and J. Tinka Gammel, *Phys. Rev.*, **B37** (1988), 6315.
[12] T. Tanaka *et al.*, *Cryst. Liq. Cryst.*, **83** (1982), 75.